

# Instrumental Processes Using Integrated Covariances

Søren Wengel Mogensen

SOREN.WENGEL.MOGENSEN@CONTROL.LTH.SE

*Department of Automatic Control, Lund University, Sweden*

**Editors:** Mihaela van der Schaar, Dominik Janzing and Cheng Zhang

## Abstract

Instrumental variable methods are often used for parameter estimation in the presence of confounding. They can also be applied in stochastic processes. Instrumental variable analysis exploits moment equations to obtain estimators for causal parameters. We show that in stochastic processes one can find such moment equations using an integrated covariance matrix. This provides new instrumental variable methods, instrumental variable methods in a class of continuous-time processes as well as a unified treatment of discrete- and continuous-time processes.

**Keywords:** instrumental variables, point processes, linear Hawkes processes, VAR(p), time series, causal inference, recurrent events

## 1. Introduction

Instrumental variable (IV) techniques have a long history in economics, engineering, and causal inference, even if each field has its own standard formulation of the IV problem (Wright, 1928; Reiersøl, 1941, 1945; Sargan, 1958; Joseph et al., 1961; Wong, 1966; Wong and Polak, 1967). Recent work (Thams et al., 2022) formulates an instrumental variable problem in a (discrete-time) time series model and provides a solution which employs conditional instruments (Brito and Pearl, 2002). Thams et al. (2022) take a *variable-centric* approach in that they identify sets of variables at different lags that satisfy conditions enabling conditional instrumental variable techniques. This paper takes a *process-centric* approach, essentially by integrating out time. The IV methods of this paper therefore only use integrated measures of covariance of stochastic processes. The distinction between variable- and process-centric will be described in more detail in Section 2.

The process-centric approach outlined in this paper is applicable to discrete-time stochastic processes and can also be applied in continuous time as we show using a class of point processes. The estimand is slightly different than in existing methods, however, the estimated parameter is easily interpretable and it summarizes the strength of the dependence between stochastic processes.

As the paper uses both discrete- and continuous-time models, we only use the term *time series* to refer to stochastic processes in discrete time. The paper is structured as follows. Section 2 describes a classical instrumental variable problem as well as the variable-centric and process-centric approaches to IV estimation in time series. Section 3 describes the causal estimands that our IV equations identify. Section 4 describes IV methods in both linear Hawkes processes and vector-autoregressive time series, however, we focus first on the time series and the description of the linear Hawkes case is found in Section 7. In both cases, we use an integrated covariance matrix to obtain new IV results and there is a strong conceptual similarity between the two, even though the interpretation of the parameters depends on the model class. We also generalize the results in the time series setting to allow more general confounding and more general instrumental processes (Section 5). Section 6 discusses estimation for time series models.

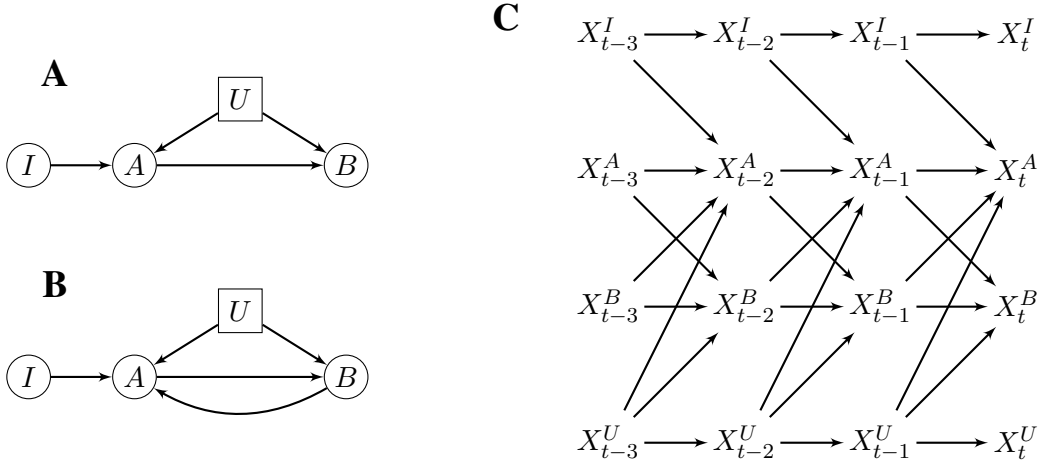


Figure 1: Graphical representations of the examples in Section 2. **A:** Graph representing the IV model in Example 1. Each node  $Y \in \{I, A, B, U\}$  represents a random variable in the model. **B:** Graph representing the time series IV model in Example 2. Each node  $Y \in \{I, A, B, U\}$  represents a coordinate process, i.e.,  $(X_t^Y)_{t \in \mathbb{Z}}$ . **C:** An *unrolled* version of **B** representing the time series IV model (Danks and Plis, 2013). Each node represents a random variable. The analogous graph with a node for every random variable in the time series is known as the *full time graph* (Peters et al., 2013).

## 2. Instrumental Variable Methods

In this section, we give an example of a classical IV problem, that is, using variables that are not indexed by time. We then compare this to a simple vector-autoregressive model of order 1, VAR(1). In this model, we explain the *variable*- and *process*-centric approaches to IV estimation and show how the integrated covariance enables IV estimation. We assume zero-mean random variables as the generalization is straightforward.

**Example 1 (Classical IV)** Assume we have observable, zero-mean random variables,  $I, A, B$ , and

$$B = \phi A + \varepsilon$$

where  $\varepsilon$  is a zero-mean random variable. We wish to estimate  $\phi \in \mathbb{R}$ . If  $\varepsilon$  and  $A$  are correlated, then least-squares estimation is biased. If  $I$  is uncorrelated with  $\varepsilon$  and  $E(AI) \neq 0$ , then we say that  $I$  is an instrumental variable. Multiplying by  $I$ , and taking expectations, we obtain

$$E(BI) = \phi E(AI). \quad (1)$$

This moment equation identifies the parameter  $\phi$  as  $E(AI) \neq 0$ . This is also true when  $A$  and  $\varepsilon$  are correlated, for instance, due to an unobserved confounder,  $U$ , see Figure 1A.

From the above it is clear that the parameter  $\phi$  is in fact identified from the covariance matrix of the vector  $(I, A, B)^T$ , that is, the observed covariance matrix is sufficient for IV estimation. The

central idea of this paper is to use a different observable matrix in a stochastic process setting which is shown to be sufficient for IV estimation. The next example illustrates this in a simple manner.

**Example 2 (Time series IV)** We consider a time series model with a structure which is similar to that in Example 1. Let  $X_t = (X_t^I, X_t^A, X_t^B, X_t^U)^T$  such that  $X_t^U$  is unobserved and processes  $X_t^I, X_t^A, X_t^B, X_t^U$  are all one-dimensional and zero-mean. For simplicity, we assume  $X_t$  to be a vector-autoregressive process of order 1 (VAR(1)),

$$X_t = \Phi X_{t-1} + \varepsilon_t,$$

where  $\varepsilon_t$  are identically distributed and independent random vectors with independent entries. The matrix  $\Phi$  has the following structure,

$$\Phi = \begin{bmatrix} \Phi_{II} & 0 & 0 & 0 \\ \Phi_{AI} & \Phi_{AA} & \Phi_{AB} & \Phi_{AU} \\ 0 & \Phi_{BA} & \Phi_{BB} & \Phi_{BU} \\ 0 & 0 & 0 & \Phi_{UU} \end{bmatrix}.$$

We assume that each entry of  $\Phi$  is nonzero if it is not explicitly zero above. There is a graphical representation of this process in Figure 1B where  $Z \rightarrow Y$  if and only if  $\Phi_{YZ} \neq 0$  for  $Z, Y \in \{I, A, B, U\}$ ,  $Z \neq Y$ . In Figure 1, graph C is an unrolled version of graph B where the nodes represent random variables and  $X_{t-1}^Z \rightarrow X_t^Y$  if and only if  $\Phi_{YZ} \neq 0$  (Danks and Plis, 2013).

If we were to apply the approach from Example 1, we could consider using  $X_{t-2}^I$  as an instrument to identify the parameter  $\Phi_{BA}$  which corresponds to the edge  $X_{t-1}^A \rightarrow X_t^B$  and write

$$\begin{aligned} X_t^B &= \Phi_{BA} X_{t-1}^A + \Phi_{BB} X_{t-1}^B + \Phi_{BU} X_{t-1}^U + \varepsilon_t^B \\ &= \Phi_{BA} X_{t-1}^A + \bar{\varepsilon}_t^B \\ E(X_t^B X_{t-2}^I) &= \Phi_{BA} E(X_{t-1}^A X_{t-2}^I) + E(\bar{\varepsilon}_t^B X_{t-2}^I) \end{aligned}$$

where  $\bar{\varepsilon}_t^B = \Phi_{BB} X_{t-1}^B + \Phi_{BU} X_{t-1}^U + \varepsilon_t^B$ . Thams et al. (2022) (Proposition 6) show that using the moment equation in (1), with  $I = X_{t-2}^I, A = X_{t-1}^A, B = X_t^B$ , does not lead to consistent estimation of  $\Phi_{BA}$  when both  $\Phi_{II}$  and  $\Phi_{BB}$  are nonzero. Therefore, naive application of classical IV methods will not give consistent estimation in this problem. This can be explained by the fact that there are confounding paths going back in time, e.g.,  $X_{t-2}^I \leftarrow X_{t-3}^I \rightarrow X_{t-2}^A \rightarrow X_{t-1}^B \rightarrow X_t^B$ , corresponding to the fact that  $E(\bar{\varepsilon}_t^B X_{t-2}^I)$  is not necessarily zero.

Thams et al. (2022) instead provide consistent estimators of  $\Phi_{BA}$  using conditional instrumental variables, using a conditional version of the moment equation in Equation (1). In this case,  $I_{t-2}$  is a conditional instrument for the parameter  $\Phi_{BA}$  conditionally on  $X_{t-3}^I$  (Thams et al., 2022, Theorem 7).

The conditional instrumental variable approach is *variable-centric* in the sense that it identifies finite sets of variables that satisfy assumptions of a conditional instrumental variable method as in the above example. In this paper, we take a different approach which will also provide a solution

to the instrumental variable problem above. Instead of looking at covariances of single variables, e.g., between  $X_t^B$  and  $X_{t-2}^I$ , we use an integrated measure of covariance, summing out temporal dependence. Taking this point of view, we arrive at an unconditional instrumental variable method in the above example, and we say that this is a *process-centric* approach as it uses the integrated covariance. The rest of this section describes this idea in the VAR(1)-example, though we no longer require  $X_t^I$ ,  $X_t^A$ ,  $X_t^B$ , and  $X_t^U$  to be one-dimensional.

Assume that the observed variables are mean-zero and that the largest absolute value of the eigenvalues of  $\Phi$  is strictly less than one. In the model from Example 2, we see that for a fixed  $t$ , and using that  $\varepsilon_{t-j}$  and  $\varepsilon_{t+k-l}$  are independent unless  $k = l - j$ ,

$$\begin{aligned} C &= \sum_{k=-\infty}^{\infty} E(X_t X_{t+k}^T) = \sum_{k=-\infty}^{\infty} E \left( \left( \sum_{j=0}^{\infty} \Phi^j \varepsilon_{t-j} \right) \left( \sum_{l=0}^{\infty} \Phi^l \varepsilon_{t+k-l} \right)^T \right) \\ &= \left( \sum_{j=0}^{\infty} \Phi^j \right) \Theta \left( \sum_{l=0}^{\infty} \Phi^l \right)^T = (I - \Phi)^{-1} \Theta (I - \Phi)^{-T} \end{aligned} \quad (2)$$

where  $\Theta$  is the diagonal covariance matrix of  $\varepsilon_t$ . This result also follows from standard VAR-process results (Brockwell and Davis, 1991, see the covariance matrix generating function). We will say that Equation (2) is the *integrated covariance equation*. More general time series models and the linear Hawkes model also satisfy this equation when the parameter matrices are given the correct interpretations. There is also a clear similarity with the parametrization of the observed covariance of a linear structural equation model as noted by Mogensen (2022) in the linear Hawkes model. Therefore, more general identification results from cyclic linear structural equation models may be used (Mogensen, 2022).

One can straightforwardly show that  $(I - \Phi_{BB})^{-1} \Phi_{BA} = C_{BI}(C_{AI})^{-1}$  when  $C_{AI}$  is invertible, thus identifying the matrix  $(I - \Phi_{BB})^{-1} \Phi_{BA}$  of *normalized parameters* (Subsection 3.2). This matrix has a clear causal interpretation, summarizing the direct influence of one subprocess on another (see Subsections 3.2 and 7.1). In the following sections, we show that this approach also applies to more general time series models as well as to linear Hawkes processes, a class of multivariate, continuous-time point processes.

### 3. Probabilistic Models

In this section, we introduce the VAR(p)-models while we defer the introduction of the *linear Hawkes processes* until Section 7. In both cases, a version of Equation (2) is satisfied which enables the instrumental variable methods of Section 4. This section also describes *normalized parameters* in more detail as these will constitute our estimands. It may seem surprising that the same instrumental variable technique applies to both time series and continuous-time point processes, however, similar parallels have been studied in other work (Brillinger, 1994). Despite the strong connections between the two settings, the linear Hawkes processes are only introduced at the end of the paper to obtain a simpler presentation. We do, however, compare the two cases throughout the paper to highlight the similarities and differences.

### 3.1. Time Series

Let  $X_t = (X_t^1, \dots, X_t^n)^T$  be a multivariate time series in discrete time,  $t \in \mathbb{Z}$ . We assume that  $X_t$  is stationary and that  $E((X_t^i)^2) < \infty$  for all  $i$  and  $t$ . We say that  $X_t$  is a VAR(p)-process if

$$X_t = \sum_{k=1}^p \Phi_k X_{t-k} + \varepsilon_t \quad (3)$$

where the  $\varepsilon$ -process is mean-zero and stationary,  $\varepsilon_t$  and  $\varepsilon_s$  are uncorrelated for  $s \neq t$ , and  $E(\varepsilon_t \varepsilon_t^T) = \Theta$ . Define  $\Phi(z) = I - \Phi_1 z - \dots - \Phi_p z^p$ . We assume that  $\det(\Phi(z)) \neq 0$  for all  $z \in \mathbb{C}$  such that  $|z| \leq 1$ . This means that there exists a unique stationary solution to the VAR(p)-equation (Brockwell and Davis, 1991, Theorem 11.3.1) and we assume throughout that we observe a stationary time series. We use the notation  $\Phi = \sum_{i=1}^p \Phi_i$ . The above assumption on  $\Phi(z)$  implies that  $I - \Phi$  is invertible. The entries of the matrix  $(I - \Phi)^{-1}$  are sometimes called *long-run effects* (Lütkepohl, 2005). We also assume that  $I - \Phi_{BB}$  is invertible when needed, see also Subsection 3.2. The *spectral radius*,  $\rho(A)$ , of a square matrix  $A$  is the largest absolute value of its eigenvalues, and we assume  $\rho(\Phi) < 1$ .

We define the *integrated covariance* of the time series  $X_t$ ,

$$C = \sum_{k=-\infty}^{\infty} E(X_t X_{t+k}^T) - E(X_t) E(X_{t+k})^T.$$

The matrix  $C$  is well-defined since the sum converges (Brockwell and Davis, 1991, p. 420). Brockwell and Davis (1991) (Section 11.2) discuss estimation of the terms  $E(X_t X_{t+k}^T)$ . The matrix  $C$  is independent of  $t$  due to stationarity. One should also note that the matrix  $C$  equals  $2\pi$  times the spectral density matrix of  $X_t - E(X_t)$  at 0.

We saw in Section 2 that the integrated covariance equation holds for VAR(1)-processes and we can extend this result to VAR(p)-processes. This is done in Appendix A. We obtain the same integrated covariance equation, however,  $\Phi$  is now the sum of the direct effects for each lag  $k = 1, \dots, p$ , that is,  $\Phi = \sum_{k=1}^p \Phi_k$ . Again, this result is also implied by textbook results on time series (Brockwell and Davis, 1991, p. 420).

We note that  $\Phi$  in the VAR(p)-case may have negative entries which is different from the linear Hawkes case. This means that some results that apply in the linear Hawkes setting do not hold in VAR(p)-time series, e.g., in relation to marginalization (Mogensen, 2022; Hyttinen et al., 2012).

### 3.2. Normalized Parameters

The entries of the parameter matrix  $\Phi$  have an intuitive interpretation. However, in general we will not be able to identify these parameters with the methods in this paper, see Example 12. Instead, we will aim to identify the entries of the *normalized* parameter matrix. These parameters also have a useful interpretation as we will explain. We use  $I_n$  to denote the identity matrix of dimension  $n$  and  $I_B$  to denote the identity matrix of dimension  $|B|$  for a finite set  $B$ .

**Definition 3 (Normalized parameters)** Consider a pair of matrices  $(\Phi, \Theta)$  that solve the integrated covariance equation. We say that they are normalized if  $\Phi_{ii} = 0$  for all  $i$ .

Say we consider any pair  $(\Phi, \Theta)$  and wish to normalize it. We define  $D$  to be the diagonal matrix such that  $D_{ii} = (1 - \Phi_{ii})^{-1}$ . Note that  $\Phi_{ii} \neq 1$  due to the assumptions on  $\Phi$  (Subsection 3.1 and Section 7). The matrix  $D$  is invertible and

$$C = (I_n - \Phi)^{-1} \Theta (I_n - \Phi)^{-T} = (D(I_n - \Phi))^{-1} D \Theta D (D(I_n - \Phi))^{-T} \quad (4)$$

$$= (I_n - \bar{\Phi})^{-1} \bar{\Theta} (I_n - \bar{\Phi})^{-T}, \quad (5)$$

$\bar{\Phi} = I_n - D(I_n - \Phi)$ . We see that  $(\bar{\Phi})_{ji} = \Phi_{ji}/(1 - \Phi_{jj})$  for  $j \neq i$  and that  $\bar{\Phi}$  has zeros on the diagonal and therefore  $(\bar{\Phi}, \bar{\Theta})$  is normalized.

In a VAR(1)-model, we see that  $(\Phi_{jj})^k \Phi_{ji}$  is the partial causal effect corresponding to the path  $X_t^i \rightarrow X_{t+1}^j \rightarrow X_{t+2}^j \rightarrow \dots \rightarrow X_{t+k+1}^j$ . If  $|\Phi_{jj}| < 1$ , we have  $\Phi_{ji}/(1 - \Phi_{jj}) = \sum_{k=0}^{\infty} (\Phi_{jj})^k \Phi_{ji}$  and the normalized parameter is therefore the sum of the partial effects (Tian, 2004) along all paths of the type  $X_t^i \rightarrow X_{t+1}^j \rightarrow X_{t+2}^j \rightarrow \dots \rightarrow X_{t+k+1}^j$  and a measure of the causal influence of the variable  $X_t^i$  on the entire future of process  $j$ , counting the direct effect as well as subsequent self-effects. The normalized parameters are seen to represent an easily interpretable causal quantity.

We will also use quantities of the type  $(I_b - \Phi_{BB})^{-1} \Phi_{BA}$  which is a multivariate version of the above. The interpretation generalizes in a straightforward manner to this case. We see that  $\Phi_{BB}^k \Phi_{BA}$  are the partial effects (Tian, 2004) from  $X_t^A$  to  $X_{t+k+1}^B$  corresponding to paths  $A \rightarrow B \rightarrow B \rightarrow \dots \rightarrow B$ . If  $\rho(\Phi_{BB}) < 1$ , this means that  $(I_b - \Phi_{BB})^{-1} \Phi_{BA} = \sum_{k=0}^{\infty} \Phi_{BB}^k \Phi_{BA}$  is an aggregate causal effect from  $X_t^A$  to  $\{X_{t+j}^B\}_{j \geq 1}$  taking only paths of the type  $A \rightarrow B \rightarrow B \rightarrow \dots \rightarrow B$  into account. In this sense, it is a direct effect of  $A$  at time  $t$  on the entire future  $B$ -process counting the direct effect  $X_t^A \rightarrow X_{t+1}^B$  and subsequent self-effects within  $B$ . Therefore, this is a natural quantification of the effect of subprocess  $A$  on subprocess  $B$  when taking a stochastic process point of view. The condition that  $\rho(\Phi_{BB}) < 1$  is a natural requirement for the above interpretation of normalized parameters as this means that the marginal  $B$ -time series is ‘stable’ in itself. This ensures that the induced self-effects are finite.

Example 12 in Appendix B shows that from a normalized pair,  $(\Phi, \Theta)$ , we can find different pairs  $(\bar{\Phi}, \bar{\Theta})$  solving the same integrated covariance equation as the original pair. If  $\rho(\Phi) < 1$  and the entries are nonnegative and we let  $0 < D_{ii} < 1$ , then the same holds for  $\bar{\Phi}$ . This means that in both the time series case and the linear Hawkes case we may find infinitely many pairs  $(\bar{\Phi}, \bar{\Theta})$  that solve the equation. In the time series case, we need to argue that  $I - \bar{\Phi}_{BB}$  is also invertible. These arguments are provided in Example 12 in Appendix B. Hyttinen et al. (2012) provide similar arguments in the context of cyclic linear structural equation models.

### 3.3. Graphical Representation

One may use graphs to represent assumptions that are sufficient for IV analysis. These graphs are defined for VAR(p)-models below.

**Definition 4 (Causal graph)** Let  $\mathcal{G}$  be a directed graph on nodes  $V$  and with edge set  $E$ . In the VAR(p)-model, we say that  $\mathcal{G}$  is the causal graph of the process if  $i \rightarrow j$  is in  $E$ ,  $i \neq j$ , if and only if there exists  $k$  such that  $(\Phi_k)_{ji} \neq 0$ .

Note that the causal graph does not contain loops, that is, edges  $i \rightarrow i$ . When identifying normalized parameters, loops are inconsequential as the normalization removes self-effects and adjusts the other parameters to retain the integrated covariance.

We say that  $i$  is a *parent* of  $j$  if  $i \rightarrow j$  in  $\mathcal{G}$ , or if  $i = j$ , and we say that a process,  $j$ , is *exogenous* if it has no parents other than  $j$  in the causal graph. We say that a subset of processes,  $I \subseteq V$ , are *exogenous* if there are no  $i \notin I$  and  $j \in I$  such that  $i \rightarrow j$  in the causal graph. Note that there could be edges between processes in an exogeneous set,  $I$ , only not from processes  $V \setminus I$  and into  $I$ .

#### 4. Instrumental Processes

We first describe the results for VAR(p)-process. The linear Hawkes setting is analogous as we will see in Section 7, though, the interpretation of the parameters differs. Section 5 provides a result for more general time series.

This section uses the algebraic equation in (2) to define instrumental processes that allow us to identify *normalized* causal parameters (see Definition 3). Mogensen (2022) notes that the parametrization of the integrated covariance is similar to the parametrization of the covariance of a linear structural equation model for which there are several identification results, see, e.g., Foygel et al. (2012); Chen (2016); Weihs et al. (2018). We will not use this connection directly and therefore we refer to that paper for a detailed explanation. One should note that identification results from linear SEMs could be used to obtain some of the results of this paper. However, we take a more direct approach which is closer to other IV work. Furthermore, this approach also makes the needed assumptions explicit whereas identification results are often only generic, that is, hold outside a measure-zero set of parameters.

The results in this section are similar in spirit to other IV work, however, we use the matrix  $C$  directly, and not a set of random variables.  $C$  is easily seen to be similar to a covariance matrix, but it is an aggregate measure of covariance between processes rather than the covariance of a set of observed random variables.

We first give a univariate definition of an instrumental process which leads to an identification result. We then define a multivariate instrumental process and state the corresponding identification result. The univariate definition and result are naturally implied by the multivariate result. However, we include them in this order to present the simplest possible setting first. The symbol  $\iota$  will throughout the paper denote an instrumental process for the effect from  $\alpha$  to  $\beta$ , where  $\iota, \alpha, \beta \in O$  and  $O \subseteq V$  is a set of observed processes. The symbol  $I$  will denote an instrumental process which is instrumental for the effect from the set  $A$  to the set  $B$ , where  $I, A, B \subseteq O$ . We assume that  $I, A$ , and  $B$  are disjoint. We say that  $\alpha$  is a *descendant* of  $\beta$  in  $\mathcal{G}$  if there exists a directed path  $\beta \rightarrow \dots \rightarrow \alpha$ . We let  $\text{deg}(\beta)$  denote the set of descendants of  $\beta$ . We let  $\text{pa}_{\mathcal{G}}(\beta)$  denote the set of parents of  $\beta$ . By convention,  $\beta \in \text{deg}(\beta)$  and  $\beta \in \text{pa}_{\mathcal{G}}(\beta)$ . We define  $\text{deg}(B) = \cup_{\beta \in B} \text{deg}(\beta)$  and  $\text{pa}_{\mathcal{G}}(B) = \cup_{\beta \in B} \text{pa}_{\mathcal{G}}(\beta)$ .

**Definition 5** Let  $\iota, \alpha$ , and  $\beta$  be distinct. We say that  $\iota$  is a VAR(p)-instrumental process for  $\alpha \rightarrow \beta$  in the causal graph  $\mathcal{G}$  if  $\iota$  is exogenous,  $\text{deg}(\iota) \cap \text{pa}_{\mathcal{G}}(\beta) \subseteq \{\alpha, \beta\}$ , and  $C_{\alpha\iota} \neq 0$ .

We will later give a more general definition of an instrumental process, and we say *instrumental process* instead of *VAR(p)-instrumental process* when it is clear from the context that we are considering a VAR(p)-model. We emphasize that  $\iota \in V$  is a *coordinate process*. In the time series case, it is the collection of random variables  $(X_t^\iota)_{t \in \mathbb{Z}}$ . Jiang et al. (2023) describe an instrumental variable method in point process models using a random variable as an instrument. In contrast, we are using an entire coordinate process as an instrument.



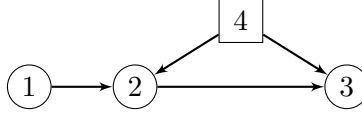


Figure 2: Instrumental process example. Each node  $\alpha$ ,  $\alpha \in \{1, 2, 3, 4\}$ , represents an entire *co-ordinate process*, that is, the collection of random variables  $(X_t^\alpha)_{t \in \mathbb{Z}}$  in the time series case. Process 4 is unobserved (indicated by the square). Process 1 ( $\iota$ ) may serve as an instrumental process to estimate the normalized effect from 2 ( $\alpha$ ) to 3 ( $\beta$ ).

One should also note that Definition 5 makes assumptions on the causal graph from Definition 4. This graph is constructed from the parameters of the time series and therefore Definition 5 also imposes restrictions on the way the coordinate processes interact.

**Theorem 6** *Let  $\mathcal{G} = (V, E)$  be a causal graph,  $V = O \dot{\cup} U$ , and let  $\iota, \alpha, \beta \in O$ . If  $\iota$  is an instrumental process for  $\alpha \rightarrow \beta$ , then  $(1 - \Phi_{\beta\beta})^{-1}\Phi_{\beta\alpha}$  is identified by  $C_{\beta\iota}/C_{\alpha\iota}$ .*

**Example 7 (Instrumental process)** *In this example, we show that the classical IV graph also allows an IV analysis in this setting. Say we have a four-dimensional VAR(1)-process such that the causal graph is as shown in Figure 2A and process 4 is unobserved. Process 1 is an instrument for  $2 \rightarrow 3$ . Theorem 6 gives that*

$$C_{3,1}/C_{2,1}$$

*identifies the normalized effect  $(1 - \Phi_{33})^{-1}\Phi_{32}$ . Section E provides an example using a VAR(2)-model and its unrolled graph.*

#### 4.1. Multiple Instruments

As in other instrumental variable frameworks, we may consider using *multiple instruments* when there are multiple processes that are instrumental for the same effects. Note that we throughout assume  $I_b - \Phi_{BB}$  to be invertible.

**Definition 8** *Let  $I, A, B \subseteq O$  be disjoint and non-empty sets. We say that a set of processes,  $I$ , is a VAR(p)-instrumental process for  $A \rightarrow B$  in the causal graph  $\mathcal{G}$  if  $I$  is exogenous,  $\deg_{\mathcal{G}}(I) \cap \text{pa}_{\mathcal{G}}(B) \subseteq A \cup B$ , and  $C_{AI}$  has full row rank.*

**Theorem 9 (Multiple instruments (just identified))** *Let  $I, A, B \subseteq O$ . If  $I$  is an instrumental process for the effect  $A \rightarrow B$  and  $|A| = |I|$ , then  $(I_b - \Phi_{BB})^{-1}\Phi_{BA}$  is identified by  $C_{BI}(C_{AI})^{-1}$ .*

If the condition  $\deg_{\mathcal{G}}(I) \cap \text{pa}_{\mathcal{G}}(B) \subseteq A \cup B$  is not satisfied, one may in some cases choose a larger  $B$  to find an instrumental process. Figure 3 gives an example of a graphical structure with a multivariate instrumental process.



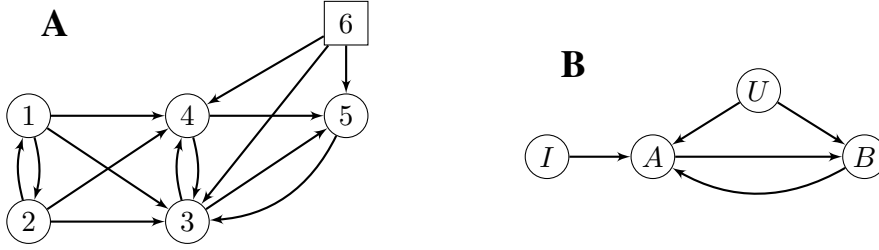


Figure 3: **A**: Multivariate instrumental process example. Process 6 is unobserved (indicated by the square). Processes 1 and 2 ( $I$ ) may serve as a multivariate instrumental process to estimate the normalized effect from 3 and 4 ( $A$ ) to 5 ( $B$ ). **B**: This graph is a simplified version of **A**. We collapse processes 1 and 2 into a single node and processes 3 and 4 into another node, defining sets  $I = \{1, 2\}$ ,  $A = \{3, 4\}$ ,  $B = \{5\}$ ,  $U = \{6\}$  where  $U$  is unobserved. For  $X, Y \in \{I, A, B, U\}$ ,  $X \neq Y$ , we include edges  $X \rightarrow Y$  if and only if  $x \rightarrow y$  for some  $x \in X$  and  $y \in Y$ . This recovers the ‘univariate’ IV structure from Figure 1B. [Thams et al. \(2022\)](#) use this graphical representation as well as the full time graphs as described below Figure 1.

#### 4.2. Overidentification

Consider instead the case where  $|A| < |I|$ , that is, overidentification. In this case,  $C_{AI}$  is not invertible. Let  $C_{AI}^-$  be a right inverse, that is,  $C_{AI}^-$  is an  $|I| \times |A|$  matrix such that  $C_{AI}C_{AI}^- = I_a$ . Such a matrix exists as  $C_{AI}$  has full row rank by assumption. Note that from this assumption it also follows that  $R_{AI}$  has full row rank when  $R = (I_n - \Phi)^{-1}$  as  $\text{rank}(AB) \leq \text{rank}(A)$  for matrices  $A$  and  $B$ . We see that  $R_{AI}^- = \Theta_{II}R_{II}C_{AI}^-$  is a right inverse of  $R_{AI}$ . We have

$$R_{BI}R_{AI}^- = C_{BI}C_{AI}^-.$$

The proof of Theorem 9 holds also in this case, showing that any choice of right inverse of  $C_{AI}$  leads to identification of the normalized parameters. Note that choosing a specific right inverse of  $C_{AI}$  specifies a choice of right inverse of  $R_{AI}$  as well – this specific right inverse is then used throughout the proof.

When  $W$  is a positive definite weight matrix then  $C_{AI}WC_{AI}^T$  is invertible using the fact that  $C_{AI}$  has full rank. We see that the matrix  $WC_{AI}^T(C_{AI}WC_{AI}^T)^{-1}$  is a right inverse of  $C_{AI}$ . This motivates using

$$C_{BI}WC_{AI}^T(C_{AI}WC_{AI}^T)^{-1}$$

as an estimate in the overidentified setting by plugging in estimated entries of  $C$ . See also [Thams et al. \(2022\)](#) and [Hall \(2005\)](#).

### 5. Time Series, General Case

We now argue that the above methods apply to time series models under far more general assumptions than those of a VAR(p)-model. It is also in this case possible to use a graph to represent the

assumptions we need for the instrumental variable method, however, we dispense with the graphical conditions in this section. We assume that  $(X_t^I, X_t^A, X_t^B, X_t^U)^T$  is a stationary process such that  $X_t^I, X_t^A, X_t^B$  are mean-zero and

$$X_t^B = \sum_{j=1}^p \Phi_{j,BA} X_{t-j}^A + \sum_{j=1}^p \Phi_{j,BB} X_{t-j}^B + g_B(\dots, X_{t-2}^U, X_{t-1}^U, \varepsilon_t^B) \quad (6)$$

where  $\Phi_{j,BA}$  and  $\Phi_{j,BB}$  are matrices of the appropriate dimensions and  $g_B$  is a function. We define  $\Phi_{BA} = \sum_{j=1}^p \Phi_{j,BA}$  and  $\Phi_{BB} = \sum_{j=1}^p \Phi_{j,BB}$ . If Equation (6) holds,  $X_t^I$  is independent of  $X^U$  and  $\varepsilon^B$  for all  $t$ ,  $(I_b - \Phi_{BB})$  is invertible,  $C_{BI}$  and  $C_{AI}$  are well-defined, and  $C_{AI}$  has full rank, then we say that  $I$  is an *instrumental process* for  $A \rightarrow B$ .

If  $(X_t^I, X_t^A, X_t^B, X_t^U)^T$  is a VAR(p)-model (under the stationarity condition of Subsection 3.1) and Definition 8 is satisfied, then  $I$  is also an instrumental process for  $A \rightarrow B$  using the above definition, and we see that the above assumptions are less restrictive than those used in the VAR(p)-setting. First, the linearity is only imposed by Equation (6) while  $I$  and  $U$  may depend nonlinearly on their own lagged values as no explicit assumptions are made on their dynamics. Second, the dependence of  $A$  on  $I$ ,  $U$ , and  $B$  may also be nonlinear. Using the above definition of an instrumental process, we obtain the next theorem.  $(C_{AI})^-$  denotes a right inverse of  $C_{AI}$ .

**Theorem 10** *If  $I$  is an instrumental process for  $A \rightarrow B$ , then  $(I_b - \Phi_{BB})^{-1} \Phi_{BA}$  is identified by  $C_{BI}(C_{AI})^-$ .*

**Proof** We prove the case  $p = 1$  while the general case is in Section C. We may write

$$\begin{aligned} E\left(X_t^B (X_{t+k}^I)^T\right) &= E\left((\Phi_{BA} X_{t-1}^A + \Phi_{BB} X_{t-1}^B + g_B(\dots, X_{t-2}^U, X_{t-1}^U, \varepsilon_t^B))(X_{t+k}^I)^T\right) \\ &= \Phi_{BA} E\left(X_{t-1}^A (X_{t+k}^I)^T\right) + \Phi_{BB} E\left(X_{t-1}^B (X_{t+k}^I)^T\right). \end{aligned}$$

We sum over  $k$  in the above expression,

$$\begin{aligned} \sum_{k=-\infty}^{\infty} E\left(X_t^B (X_{t+k}^I)^T\right) &= \sum_{k=-\infty}^{\infty} \Phi_{BA} E\left(X_{t-1}^A (X_{t+k}^I)^T\right) + \sum_{k=-\infty}^{\infty} \Phi_{BB} E\left(X_{t-1}^B (X_{t+k}^I)^T\right) \\ C_{BI} &= \Phi_{BA} C_{AI} + \Phi_{BB} C_{BI} \end{aligned}$$

and isolating  $C_{BI}$  we obtain  $C_{BI} = (I_b - \Phi_{BB})^{-1} \Phi_{BA} C_{AI}$ . If  $C_{AI}$  has full row rank this gives identification of the matrix  $(I_b - \Phi_{BB})^{-1} \Phi_{BA}$ . ■

One can use conditions such as those in the VAR(p)-models to ensure that the relevant entries of  $C$  are well-defined.

## 6. Estimation

In order to use the instrumental process framework above, one can estimate the relevant entries of the integrated covariance matrix and then plug in the estimated covariances to obtain estimates of the normalized parameters directly from the identifying formulas. To estimate the matrix  $C$  in the time series case, one may use the relation to the spectral density matrix of the time series, see, e.g., [Hansen \(1982\)](#); [Brillinger \(1981\)](#). One may also use the connection to *long-run covariance* to estimate  $C$ , see, e.g., [Andrews \(1991\)](#); [Andrews and Monahan \(1992\)](#).

Section D contains numerical examples of the instrumental process method in this paper. Subsection 7.1 describes estimation in the linear Hawkes case.

## 7. Linear Hawkes Processes

A *linear Hawkes process* is a certain kind of *point process*. We give a short introduction here, see also, e.g., [Laub et al. \(2015\)](#); [Daley and Vere-Jones \(2003\)](#). We consider a filtered probability space  $(\Omega, \mathcal{F}, (\mathcal{F}_t), P)$  where  $(\mathcal{F}_t)$  is a filtration and an index set  $V = \{1, 2, \dots, n\}$ . For  $i \in V$ , there is a sequence of random event times  $\{T_k^i\}_{k \in \mathbb{Z}}$  such that  $T_k^i < T_{k+1}^i$  almost surely. We define a counting process  $N_t^i$  such that  $N_t^i - N_s^i = \sum_k \mathbb{1}_{s < T_k^i \leq t}$ . Furthermore, we assume that two events cannot occur simultaneously in the multivariate point process. A linear Hawkes process can be defined by imposing constraints on the *conditional intensities*,  $\lambda_t^i$ . These are stochastic processes and satisfy

$$\lambda_t^i = \lim_{h \downarrow 0} \frac{1}{h} P(N_{t+h}^i - N_t^i = 1 \mid \mathcal{F}_t)$$

where  $\mathcal{F}_t$  represents the history of the process until time point  $t$ . A multivariate *linear Hawkes process* is a point process such that

$$\lambda_t^j = \mu_j + \sum_{i=1}^n \int_{-\infty}^t \phi_{ji}(t-s) dN_s^i$$

for a nonnegative constant  $\mu_j$  and nonnegative functions  $\phi_{ji}$  which are zero outside  $(0, \infty)$ . We assume  $\mu_j > 0$ . We define  $\Phi$  to be the  $n \times n$  matrix such that  $\Phi_{ji} = \int_{-\infty}^{\infty} \phi_{ji}(s) ds$ . See Figure 4 for an illustration of data from a linear Hawkes process. When  $A$  is a square matrix, we let  $\rho(A)$  denote its *spectral radius*, that is, the largest absolute value of its eigenvalues. We assume that  $\rho(\Phi) < 1$  in which case we can assume the linear Hawkes process to have stationary increments ([Jovanović et al., 2015](#)). We define the integrated covariance in this setting,

$$C_{ij} dt = \int_{-\infty}^{\infty} E(dN_t^i dN_{t+s}^j) - E(dN_t^i) E(dN_{t+s}^j) ds. \quad (7)$$

We define  $\Lambda_i dt = E(dN_t^i)$  and let  $\Theta$  denote the diagonal matrix such that  $\Theta_{ii} = \Lambda_i$ . It holds that

$$C = (I_n - \Phi)^{-1} \Theta (I_n - \Phi)^{-T}, \quad (8)$$

see [Achab et al. \(2017\)](#). This is the same equation as in the VAR(1)-case in Section 2, even though interpretations of the parameter matrices  $\Phi$  and  $\Theta$  differ. The following definition is analogous to Definition 4.

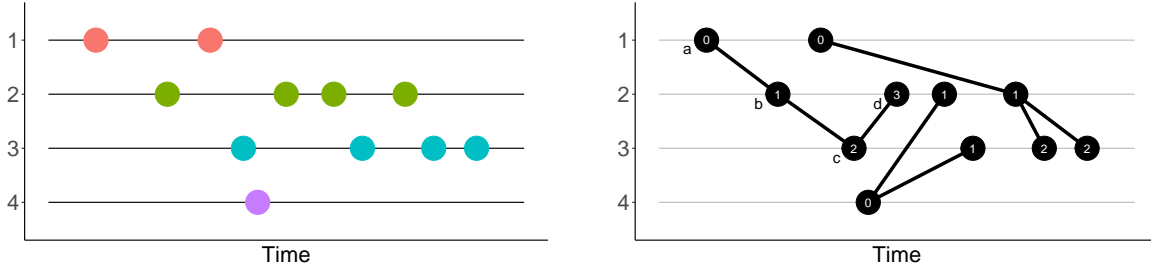


Figure 4: Example data from a four-dimensional linear Hawkes process. Left: Example observed data. Color and vertical placement indicate coordinate process (1, 2, 3, or 4) of the event. Horizontal placement indicates time of the event. Right: The linear Hawkes process can be generated as a *cluster process* where each event may spark future child events, indicated here with line segments. These parent-child relations are unobserved. In the cluster with labeled events ( $a, b, c, d$ ), event  $b$  is in the first generation after event  $a$  while event  $d$  is in the third generation after event  $a$ . We say that  $b$  is a *child* of  $a$  (direct descendant).

**Definition 11 (Causal graph)** Let  $\mathcal{G}$  be a directed graph on nodes  $V$  and with edge set  $E$ . In the linear Hawkes case, we say that  $\mathcal{G}$  is the causal graph of the process if  $i \rightarrow j$  is in  $E$ ,  $i \neq j$ , if and only if  $\Phi_{ji} \neq 0$ .

**Cluster Interpretation** Above we introduced the linear Hawkes process as a point process with conditional intensities of a certain type. It is, however, possible to give an equivalent definition using the so-called *cluster representation* (Jovanović et al., 2015). We will give a very short description here. For each  $i \in V$ , a set of generation-0 events are generated from a homogeneous Poisson process with rate  $\mu_i$ . Each of these events create a *Hawkes cluster* which is generated in the following way. From a generation- $k$  event of type  $i$  at time  $s$  (coordinate process  $i$ ), generation- $(k+1)$  events of type  $j$  are generated from an inhomogenous Poisson process started at  $s$  with rate  $\phi_{ji}(t-s)$ ,  $t > s$ . This construction is repeated. The superposition of all clusters form a linear Hawkes process. Note that only event types and time points are observed while generation and parent-child relations of an event are unknown when observing data from a linear Hawkes process.

The cluster interpretation provides a straightforward interpretation of the entries of  $\Phi$ . The entry  $\Phi_{ji}$  is the expected number of direct  $j$ -children from an  $i$ -event. In general,  $(\Phi^k)_{ji}$  is the expected number of  $j$ -events from an  $i$ -event in the  $k$ 'th generation from the  $i$ -event. We define  $R = (I_n - \Phi)^{-1} = \sum_{k=0}^{\infty} \Phi^k$ .  $R_{ji}$  is the expected total number of  $j$ -descendants on a cluster rooted at an  $i$ -event. The infinite sum converges and  $R$  is well-defined due to the assumption on the spectral radius of  $\Phi$  (Jovanović et al., 2015). See Figure 4 for an example of (in)direct descendant events.

### 7.1. Normalized Parameters

We can normalize the parameters of Equation (8) just as we did in Equation (5). In the linear Hawkes process, the normalized parameter  $\bar{\Phi}_{ji}$  is the expected number of  $j$ -events on a cluster rooted at an  $i$ -event counting only subtrees of the form  $i - j - j - \dots - j$  for any number of  $j$ -events. This is

thus the expected number of direct  $j$ -events from an  $i$ -event when also counting subsequent ‘self-events’  $j - j$ . It is clear from Equation (8) that the results in Section 4 also hold for linear Hawkes processes. If  $\rho(\Phi) < 1$  and the entries of  $\Phi$  are nonnegative, then this will also be the case for  $\bar{\Phi}$  in Equation (5) (Mogensen, 2022). This means that the normalized parameters are also within the Hawkes parameter space.

## 7.2. Estimation

Achab et al. (2017) describe how to estimate cumulants of linear Hawkes process. We sketch their approach below. We assume that we observe a linear Hawkes process over the interval  $[0, T]$  and that there exists  $H > 0$  such that restricting the integration in Equation (7) to  $[-H, H]$  introduces only a negligible error. As pointed out by Achab et al. (2017), this is reasonable if the support of  $\phi_{ji}$  is small compared to  $H$  and the spectral radius of  $\Phi$  is sufficiently small. Given a realization of a stationary linear Hawkes process on  $[0, T]$  let  $p_i = \{t_1^i, \dots, t_{m_i}^i\} \subset [0, T]$  be the observed event times of process  $i$ . The following are estimators of the first- and second-order cumulants,

$$\hat{\Lambda}_i = \frac{1}{T} \sum_{k=1}^{m_i} 1, \quad \hat{C}_{ij} = \frac{1}{T} \sum_{k=1}^{m_i} \left( N_{t_k^i+H}^j - N_{t_k^i-H}^j - 2H\hat{\Lambda}^j \right)$$

In the above,  $N_t^i$  refers to the observed counting process corresponding to process  $i$ , that is,  $N_t^i = 0$  for  $t < 0$  and in general  $N_t^i = \sum_{k=1}^{m_i} \mathbb{1}_{t_k^i \leq t}$ . As noted by Achab et al. (2017), there is a bias in the estimation of the integrated covariance, however, it is found to be negligible. Achab et al. (2017) (Theorem 2.1 and Remark 1) show asymptotic consistency for  $H_T \rightarrow \infty$  and  $H_T^2/T \rightarrow 0$  where  $H_T$  is the value of the parameter  $H$  used when observing the process on the interval  $[0, T]$ .

## 8. Conclusion

The instrumental variable method in this paper provides a moment equation for time series models which avoids using a conditional moment equation as in Thams et al. (2022). It also makes minimal assumptions on the marginal distribution of the instrumental process. On the other hand, it involves an integral or an infinite sum which needs to be estimated when applying the method. One should also note that our estimands are slightly different than those of Thams et al. (2022). As shown, the estimands in this paper do have a simple causal interpretation, however.

The integrated covariance approach also allows a unified treatment of IV methods in time series (discrete-time) and continuous-time processes as illustrated by the application to the continuous-time linear Hawkes processes. It is clearly of interest to extend this framework to more general classes of continuous-time processes. Finally, one should also note that the parametrization of the integrated covariance can be used to obtain other identification results than the instrumental variable results in this paper.

## Acknowledgments

This work was supported by a DFF-International Postdoctoral Grant (0164-00023B) from Independent Research Fund Denmark. The author is a member of the ELLIIT Strategic Research Area at Lund University. The author thanks Nikolaj Thams and Jonas Peters for helpful discussions. The author is also grateful to the reviewers for their constructive comments and suggestions.

## References

- Massil Achab, Emmanuel Bacry, Stéphane Gaïffas, Iacopo Mastromatteo, and Jean-François Muzy. Uncovering causality from multivariate Hawkes integrated cumulants. In *Proceedings of the 34th International Conference on Machine Learning (ICML)*, 2017.
- Donald WK Andrews. Heteroskedasticity and autocorrelation consistent covariance matrix estimation. *Econometrica*, 59(3):817–858, 1991.
- Donald WK Andrews and J Christopher Monahan. An improved heteroskedasticity and autocorrelation consistent covariance matrix estimator. *Econometrica*, 60(4):953–966, 1992.
- David R Brillinger. *Time Series: Data Analysis and Theory*. Holden Day, Inc., San Francisco, 1981.
- David R Brillinger. Time series, point processes, and hybrids. *Canadian Journal of Statistics*, 22(2):177–206, 1994.
- Carlos Brito and Judea Pearl. Generalized instrumental variables. In *Proceedings of the Eighteenth conference on Uncertainty in Artificial Intelligence (UAI)*, 2002.
- Peter J Brockwell and Richard A Davis. *Time Series: Theory and Methods*. Springer, New York, 2nd edition, 1991.
- Bryant Chen. Identification and overidentification of linear structural equation models. In *Advances in Neural Information Processing Systems*, volume 29, 2016.
- Daryl J Daley and David Vere-Jones. *An Introduction to the Theory of Point Processes*. Springer, New York, 2nd edition, 2003.
- David Danks and Sergey Plis. Learning causal structure from undersampled time series. In *NIPS 2013 Workshop on Causality*, 2013.
- Rina Foygel, Jan Draisma, and Mathias Drton. Half-trek criterion for generic identifiability of linear structural equation models. *The Annals of Statistics*, 40(3):1682–1713, 2012.
- Alastair R Hall. *Generalized method of moments*. Oxford University Press, 2005.
- Lars Peter Hansen. Large sample properties of generalized method of moments estimators. *Econometrica*, 50(4):1029–1054, 1982.
- Roger A Horn and Charles R Johnson. *Matrix Analysis*. Cambridge University Press, 1985.
- Antti Hyttinen, Frederick Eberhardt, and Patrik O Hoyer. Learning linear cyclic causal models with latent variables. *The Journal of Machine Learning Research*, 13(1):3387–3439, 2012.
- Zhichao Jiang, Shizhe Chen, and Peng Ding. An instrumental variable method for point processes: generalized Wald estimation based on deconvolution. *Biometrika*, 2023. To appear.
- P Joseph, J Lewis, and J Tou. Plant identification in the presence of disturbances and application to digital adaptive systems. *Transactions of the American Institute of Electrical Engineers, Part II: Applications and Industry*, 80(1):18–24, 1961.

- Stojan Jovanović, John Hertz, and Stefan Rotter. Cumulants of Hawkes point processes. *Physical Review E*, 91(4):042802, 2015.
- Patrick J Laub, Thomas Taimre, and Philip K Pollett. Hawkes processes. *arXiv:1507.02822*, 2015.
- Helmut Lütkepohl. *New Introduction to Multiple Time Series Analysis*. Springer, Berlin, 2005.
- Søren Wengel Mogensen. Equality constraints in linear Hawkes processes. In *Proceedings of the 1st Conference on Causal Learning and Reasoning (CLear)*, 2022.
- Jonas Peters, Dominik Janzing, and Bernhard Schölkopf. Causal inference on time series using restricted structural equation models. In *Advances in Neural Information Processing Systems*, volume 26, 2013.
- R Core Team. *R: A Language and Environment for Statistical Computing*. R Foundation for Statistical Computing, Vienna, Austria, 2021. URL <https://www.R-project.org/>.
- Olav Reiersøl. Confluence analysis by means of lag moments and other methods of confluence analysis. *Econometrica*, 9(1):1–24, 1941.
- Olav Reiersøl. *Confluence analysis by means of instrumental sets of variables*. PhD thesis, Stockholms Höskola, 1945.
- John D Sargan. The estimation of economic relationships using instrumental variables. *Econometrica*, 26(3):393–415, 1958.
- Nikolaj Thams, Rikke Søndergaard, Sebastian Weichwald, and Jonas Peters. Identifying causal effects using instrumental time series: Nuisance IV and correcting for the past. *arXiv:2203.06056*, 2022.
- Jin Tian. Identifying linear causal effects. In *Proceedings of the 19th AAAI Conference on Artificial Intelligence*, 2004.
- Luca Weihs, Bill Robinson, Emilie Dufresne, Jennifer Kenkel, Kaie Kubjas, Reginald McGee II, Nhan Nguyen, Elina Robeva, and Mathias Drton. Determinantal generalizations of instrumental variables. *Journal of Causal Inference*, 6(1), 2018.
- K Y Wong. *Estimation of parameters of linear systems using the instrumental variable method*. PhD thesis, University of California, Berkeley, 1966.
- Kwan Wong and Elijah Polak. Identification of linear discrete time systems using the instrumental variable method. *IEEE Transactions on Automatic Control*, 12(6):707–718, 1967.
- Philip G Wright. *Tariff on animal and vegetable oils*. Macmillan Company, New York, 1928.
- Riadh Zaatour. *hawkes: Hawkes process simulation and calibration toolkit*, 2014. URL <https://CRAN.R-project.org/package=hawkes>. R package version 0.0-4.
- Achim Zeileis, Susanne Köll, and Nathaniel Graham. Various versatile variances: An object-oriented implementation of clustered covariances in R. *Journal of Statistical Software*, 95(1): 1–36, 2020. doi: 10.18637/jss.v095.i01.



## Appendix A. Integrated Covariance, VAR(p)

First, we rewrite the VAR(p)-process as a VAR(1)-process,  $Y$ , with  $np$  coordinate processes,

$$Y_t = \Phi_Y Y_{t-1} + \varepsilon_t^Y = \begin{bmatrix} \Phi_1 & \Phi_2 & \dots & \Phi_{p-1} & \Phi_p \\ I & 0 & \dots & 0 & 0 \\ 0 & I & \dots & 0 & 0 \\ \vdots & \vdots & \ddots & \vdots & \vdots \\ 0 & 0 & \dots & I & 0 \end{bmatrix} Y_{t-1} + \begin{bmatrix} \varepsilon_t \\ 0 \\ 0 \\ \vdots \\ 0 \end{bmatrix}$$

The VAR(1)-computations from above still hold which means that the integrated covariance of  $Y$  can be written as

$$C_Y = (I_{np} - \Phi_Y)^{-1} \Theta_Y (I_{np} - \Phi_Y)^{-T}.$$

Note that if 1 is an eigenvalue of  $\Phi_Y$ , then it corresponds to an eigenvector which is the concatenation of  $p$  copies of a single  $n$ -vector. This  $n$ -vector is also an eigenvector of  $\Phi = \sum_{i=1}^p \Phi_i$  with eigenvalue 1 which is a contradiction. This means that  $I_{np} - \Phi_Y$  is invertible. We can use Schur complements and the structure of  $(I_{np} - \Phi_Y)$  to see that  $((I_{np} - \Phi_Y)^{-1})_{1:n,1:n} = (I_n - \Phi)^{-1}$  where  $\Phi = \sum_{i=1}^p \Phi_i$ . From the sparsity of  $\Theta_Y$  it follows that

$$C = (C_Y)_{1:n,1:n} = (I_n - \Phi)^{-1} \Theta (I_n - \Phi)^{-T}.$$

## Appendix B. Normalization

**Example 12** Consider a representation such that  $\Phi$  is normalized (i.e., has zeros on the diagonal)

$$C = (I_n - \Phi)^{-1} \Theta (I_n - \Phi)^{-T}.$$

For any diagonal matrix such that  $D_{ii} \neq 1$  for all  $i$ ,

$$C = (D(I_n - \Phi))^{-1} D \Theta D (D(I_n - \Phi))^{-T} = (I_n - \bar{\Phi})^{-1} \bar{\Theta} ((I_n - \bar{\Phi}))^{-T}.$$

If  $0 < D_{ii} < 1$ ,  $\Phi$  is nonnegative, and  $\rho(\Phi) < 1$ , we show that  $\rho(\bar{\Phi}) < 1$ . To see this note that  $\bar{\Phi} = I_n - D + D\Phi$ . This is a nonnegative matrix and let  $\lambda = \rho(\bar{\Phi})$ . A nonzero vector  $x$  with nonnegative entries can be chosen such that  $\bar{\Phi}x = \lambda x$  ([Horn and Johnson, 1985, Theorem 8.3.1](#)).  $\Phi$  and  $x$  have nonnegative entries and  $x$  is nonzero and therefore  $\Phi x \geq x$  (the inequalities are to be read entrywise) implies that  $\rho(\Phi) \geq 1$  ([Horn and Johnson, 1985, Theorem 8.3.2](#)) so  $(\Phi x)_i < x_i$  for some  $i$ . We have  $\lambda x = (I_n - D + D\Phi)x$  and therefore  $(\lambda x)_i < x_i$  so  $\lambda < 1$ . We see that  $D\Theta D$  is positive definite. This shows that we cannot identify unnormalized direct effects from the integrated covariance matrix as every nonzero entry of  $\bar{\Phi}$  is different from the corresponding entry of  $\Phi$  (note the diagonal of  $\bar{\Phi}$  is nonzero),

$$\bar{\Phi}_{ii} = 1 - D_{ii} + \sum_k D_{ik} \Phi_{ki} = 1 - D_{ii} > 0$$

and for  $i \neq j$ ,

$$\bar{\Phi}_{ij} = \sum_k D_{ik} \Phi_{kj} = D_{ii} \Phi_{ij} < \Phi_{ij}$$

when  $\Phi_{ij} \neq 0$ .

For the time series case, note also that

$$\bar{\Phi}_{BB} = I_b - D_{BB} + (D\Phi)_{BB} = I_b - D_{BB} + D_{BB}\Phi_{BB}$$

and when  $x$  is a nonzero vector such that  $x = \bar{\Phi}_{BB}x$  then

$$x = \bar{\Phi}_{BB}x = (I_b - D_{BB} + D_{BB}\Phi_{BB})x$$

This implies  $D_{BB}x = D_{BB}\Phi_{BB}x$  and  $x = \Phi_{BB}x$  so 1 is an eigenvalue of  $\Phi_{BB}$  and therefore  $I_b - \Phi_{BB}$  is not invertible which is a contradiction. Therefore 1 is also not an eigenvalue of  $\bar{\Phi}_{BB}$  and it follows that  $I_b - \bar{\Phi}_{BB}$  is invertible.

### Appendix C. Proofs

**Proof** [Theorem 6] We have  $\rho(\Phi) < 1$ , and we define  $R = (I_n - \Phi)^{-1} = \sum_{k=0}^{\infty} \Phi^k$ . As  $\iota$  is exogenous, we have that  $C_{\alpha\iota} = R_{\iota\iota}\Theta_{\iota\iota}R_{\alpha\iota}$  and  $C_{\beta\iota} = R_{\iota\iota}\Theta_{\iota\iota}R_{\beta\iota}$ . From the definition of an instrumental process, we have  $C_{\alpha\iota} \neq 0$  and  $R_{\alpha\iota} \neq 0$ , and therefore  $R_{\beta\iota}/R_{\alpha\iota}$  is identified. Using that  $\iota$  is an instrumental process and the fact that  $I_n = (I_n - \Phi)R$ , it follows that  $R_{\beta\iota} = \Phi_{\beta\alpha}R_{\alpha\iota} + \Phi_{\beta\beta}R_{\beta\iota}$ . Therefore  $R_{\beta\iota}/R_{\alpha\iota} = \Phi_{\beta\alpha}/(1 - \Phi_{\beta\beta})$ . ■

**Proof** [Theorem 9] From exogeneity of  $I$ , it holds that  $C_{BI} = R_{BI}\Theta_{II}R_{II}$  and  $C_{AI} = R_{AI}\Theta_{II}R_{II}$ . The matrix  $C_{AI}$  has full rank and it is therefore invertible since  $|A| = |I|$ . Matrices  $R_{AI}$ ,  $\Theta_{II}$ , and  $R_{II}$  are therefore also invertible. In that case,

$$R_{BI}(R_{AI})^{-1} = C_{BI}(C_{AI})^{-1}$$

and therefore  $R_{BI}(R_{AI})^{-1}$  is identified. From the definition of  $R$ , we see that  $I_n = (I_n - \Phi)R$  and therefore  $R = I_n + \Phi R$ . This means that

$$R_{BI} = \sum_C \Phi_{BC} R_{CI} = \Phi_{BA} R_{AI} + \Phi_{BB} R_{BI}.$$

The last equality uses that  $I$  is an instrumental process. We obtain

$$R_{BI}(R_{AI})^{-1} = (I_b - \Phi_{BB})^{-1} \Phi_{BA}.$$

Note that  $R_{AI}$  is invertible as noted as above. In the linear Hawkes case, it holds that  $\rho(\Phi_{BB}) \leq \rho(\Phi) < 1$  (Horn and Johnson, 1985, Corollary 8.1.20) so  $I_b - \Phi_{BB}$  is also invertible. ■

**Proof** [Proof of Theorem 10, general  $p$ ]

We see that

$$E(X_t^B (X_{t+k}^I)^T) = E \left( \left( \sum_j \Phi_{j,BA} X_{t-j}^A + \sum_j \Phi_{j,BB} X_{t-j}^B + g_B(\dots, X_{t-2}^U, X_{t-1}^U, \varepsilon_t^U) \right) (X_{t+k}^I)^T \right).$$

We sum over  $k$ ,

$$\begin{aligned} \sum_{k=-\infty}^{\infty} E(X_t^B (X_{t+k}^I)^T) &= \sum_j \Phi_{j,BA} \sum_{k=-\infty}^{\infty} E(X_{t-j}^A (X_{t+k}^I)^T) \\ &\quad + \sum_j \Phi_{j,BB} \sum_{k=-\infty}^{\infty} E(X_{t-j}^B (X_{t+k}^I)^T) \\ &= \sum_j \Phi_{j,BA} \sum_{k=-\infty}^{\infty} E(X_t^A (X_{t+k}^I)^T) \\ &\quad + \sum_j \Phi_{j,BB} \sum_{k=-\infty}^{\infty} E(X_t^B (X_{t+k}^I)^T). \end{aligned}$$

From this it follows that  $C_{BI} = (I_b - \Phi_{BB})^{-1} \Phi_{BA} C_{AI}$ . ■

## Appendix D. Numerical Examples

We list results from numerical experiments in this section. In Experiments E1-E7 we generated observations from a single time series of length  $N$  and estimated the normalized parameter(s) using the plug-in estimator (see Section 6). We repeated this  $m$  times. Table 1 reports empirical mean squared error (MSE),  $(1/m) \cdot \sum_{i=1}^m \|\hat{\theta}_i^j - \theta_i^j\|^2$ , where  $\|\cdot\|$  is the Euclidean norm,  $\theta_i^j$  is the true normalized parameter(s) in the  $i$ 'th run of the  $j$ 'th experiment, and  $\hat{\theta}_i^j$  is its estimate. Experiment H1 is a linear Hawkes example. The causal graphs do not include loops,  $\alpha \rightarrow \alpha$ , but note that all diagonal parameters, e.g., the diagonal of  $\Phi$  in a VAR(1)-process, were nonzero. In the time series experiments, we used the `sandwich` package in R to estimate the long-run covariance (Zeileis et al., 2020; R Core Team, 2021).

**Experiment E1** Four-dimensional VAR(1)-process corresponding to graph **A** in Figure 2. Nonzero, nondiagonal VAR(1)-parameters were sampled uniformly in  $[-1, -0.2] \cup [0.2, 1]$ . Diagonal parameters were nonzero and sampled uniformly in  $[-0.5, .5]$ . The parameters were sampled repeatedly until parameters satisfying the stability condition of Subsection 3.1 were obtained.

**Experiment E2** Four-dimensional VAR(1)-process corresponding to graph **B** in Figure 1. Nonzero parameters were sampled as in Experiment E1.

**Experiment E3** Six-dimensional VAR(1)-process corresponding to graph **A** in Figure 6. Nonzero parameters were sampled as in Experiment E1. The set  $\{1, 2\}$  is instrumental for the effect from  $\{3, 4\}$  to 5.

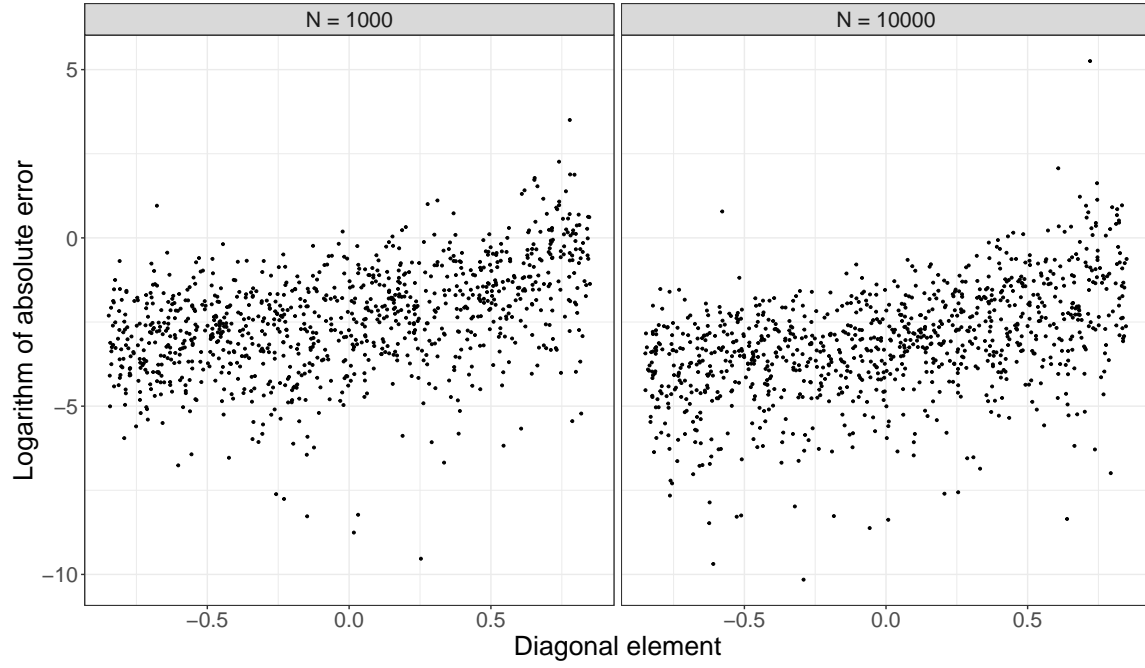


Figure 5: Results from Experiment E7. The vertical axis is the logarithm of  $|\hat{\theta}_i^7 - \theta_i^7|$ . The horizontal axis is  $\Phi_{BB}$ ,  $B = \{3\}$ . As expected from the identifying formula, estimation accuracy deteriorates when this value increases as also reflected in E7 in Table 1. Note that Experiments E1 and E7 are identical except for the fact that the diagonal elements are sampled from a larger interval in E7. This leads to smaller denominators in the definition of the normalized parameter(s) and worse estimation using a naive estimator.



Figure 6: Graphs from Experiments E3 (graph **A**) and E4 (graph **B**) in Section D. Square nodes correspond to unobserved processes.

	N	m	MSE	R
E1	1000	100	0.027	$[-1.57, 1.45]$
	10000	100	0.012	$[-1.28, 1.63]$
E2	1000	100	0.072	$[-1.38, 1.58]$
	10000	100	0.005	$[-1.38, 1.23]$
E3	1000	100	0.955	$[-1.70, 1.72]$
	10000	100	0.061	$[-1.68, 1.80]$
E4	1000	100	0.055	$[-1.39, 1.44]$
	10000	100	0.004	$[-1.35, 1.86]$
E5	1000	100	0.434	$[-5.04, 6.99]$
	10000	100	0.214	$[-11.16, 8.94]$
E6	1000	100	0.203	$[1.25, 1.25]$
	10000	100	0.020	$[1.25, 1.25]$
E7	1000	1000	1.606	$[-5.280, 6.251]$
	10000	1000	36.803	$[-6.507, 5.276]$
H1		500	0.039	$[0.26, 0.96]$

Table 1: Results from the experiments described in Section D.  $N$  is the length of the observed time series from which the estimate is computed and  $m$  is the number of repetitions.  $R$  is the range of the true normalized parameter(s) over the  $m$  runs of each experiment. The true normalized parameter was fixed in Experiment E6. We see reasonably good performance, except for E7 where a larger sampling interval for diagonal elements creates very large errors in some instances (see Figure 5).

**Experiment E4** Five-dimensional VAR(1)-process corresponding to graph **B** in Figure 6. Nonzero parameters were sampled as in Experiment E1. The set  $\{1, 2\}$  is instrumental for the effect from 3 to 4. We used  $W = I_2$ .

**Experiment E5** Four-dimensional VAR(2)-process corresponding to graph **A** in Figure 2. Nonzero parameters were sampled as in Experiment E1 and sampling was repeated until the parameters satisfied  $(\Phi_1 + \Phi_2)_{21} \geq 0.2$  and the signs of  $(\Phi_1)_{21}$  and  $(\Phi_2)_{21}$  were equal.

**Experiment E6** Four-dimensional time series corresponding to the framework in Section 5. Variables  $\varepsilon_t^I, \varepsilon_t^A, \varepsilon_t^B$ , and  $\varepsilon_t^U$  were sampled as independent Gaussian variables with a standard deviation of 0.25. For each  $t$ , data was generated as

$$\begin{aligned} X_t^I &= -\frac{1}{1 + (X_{t-1}^I)^2} + \varepsilon_t^I, \\ X_t^U &= \frac{\exp(X_{t-1}^U)}{1 + \exp(X_{t-1}^U)} + \varepsilon_t^U, \\ X_t^A &= -\frac{3}{1 + \exp(X_{t-1}^I)} - 0.5 \cdot X_{t-1}^A + X_{t-1}^U \cdot \varepsilon_t^A, \\ X_t^B &= 0.5 \cdot X_{t-1}^A + 0.6 \cdot X_{t-1}^B + X_{t-1}^U \cdot \varepsilon_t^B. \end{aligned}$$

**Experiment E7** Four-dimensional VAR(1)-process corresponding to graph **A** in Figure 2. Nonzero, nondiagonal parameters were sampled as in Experiment E1. Diagonal parameters were nonzero and sampled uniformly in  $[-0.85, .85]$ .

**Experiment H1** We generated observations from a linear Hawkes process corresponding to graph **A** in Figure 2 using the `hawkes` package in R (Zaatour, 2014; R Core Team, 2021). In their parametrization,  $\beta$ -parameters were equal to 1, and we sampled  $\alpha$ -parameters uniformly on  $[0.2, 0.5]$ . In a single run, each coordinate process had between 10000 and 40000 events.

## Appendix E. A VAR(2)-example

We give an example of a VAR(2)-process satisfying the assumptions of the instrumental process method (see also Figure 7). We assume that  $X_t = (X_t^1, X_t^2, X_t^3, X_t^4)^T$  is a VAR(2)-process such that

$$X_t = \Phi_1 X_{t-1} + \Phi_2 X_{t-2} + \varepsilon_t \quad (9)$$

$$= \begin{bmatrix} \Phi_{11}^1 & 0 & 0 & 0 \\ \Phi_{21}^1 & \Phi_{22}^1 & \Phi_{23}^1 & \Phi_{24}^1 \\ 0 & \Phi_{32}^1 & \Phi_{33}^1 & \Phi_{34}^1 \\ 0 & 0 & 0 & \Phi_{44}^1 \end{bmatrix} X_{t-1} + \begin{bmatrix} \Phi_{11}^2 & 0 & 0 & 0 \\ \Phi_{21}^2 & 0 & 0 & 0 \\ 0 & 0 & 0 & \Phi_{34}^2 \\ 0 & 0 & 0 & \Phi_{44}^2 \end{bmatrix} X_{t-2} + \varepsilon_t. \quad (10)$$

We use  $\Phi_{ij}^k$  to denote the  $(i, j)$ -entry of  $\Phi_k$ . Matrices  $\Phi_1$  and  $\Phi_2$  are as defined in (10) and  $\Phi_k = 0$  for all  $k \neq 1, 2$ . Graph **B** in Figure 7 has an edge  $X_{k_1}^i \rightarrow X_{k_2}^j$  if  $\Phi_{ji}^{k_2-k_1}$  may be nonzero. Graph **A** is a rolled version of graph **B** and we have that  $i \rightarrow j$  in graph **A**,  $i \neq j$ , if and only if there exists  $k_1$

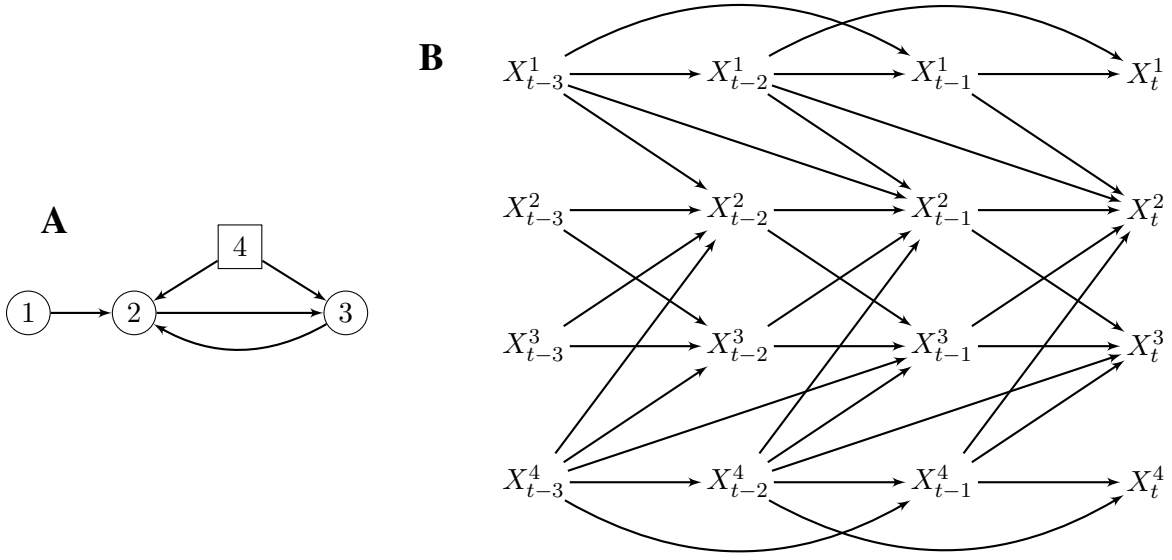


Figure 7: Graphs from the example in Section E. Process 4 is unobserved.

and  $k_2$  such that  $X_{k_1}^i \rightarrow X_{k_2}^j$  in graph **B**. Let  $\Phi = \Phi_1 + \Phi_2$ . We see that process 1 is an instrumental process for  $2 \rightarrow 3$  (Definition 5), and this means that  $\Phi_{32}/(1 - \Phi_{33})$  is identified from the observed integrated covariance if  $C_{21} \neq 0$ .